geosciences

MDPI

Article

Unraveling the Drivers Controlling the Transient and Seasonal CO_2 Dynamic in a Shallow Temperate Cave

Angel Fernandez-Cortes [1], Tamara Martin-Pozas [2], Soledad Cuezva [3], Juan Carlos Cañaveras [4], Cesareo Saiz-Jimenez [5,*] and Sergio Sanchez-Moral [2]

[1] Department of Biology and Geology, Building CITE IIB, Universidad de Almería, Carretera de Sacramento s.n, La Cañada de San Urbano, 04120 Almería, Spain
[2] Department of Geology, MNCN-CSIC, José Gutiérrez Abascal, 2, 28006 Madrid, Spain
[3] Department of Geology, Geography and Environment, University of Alcalá de Henares, Scientific Technological Campus, 28802 Alcalá de Henares, Spain
[4] Department of Environmental and Earth Sciences, University of Alicante, Campus San Vicente del Raspeig, 03690 Alicante, Spain
[5] Department of Agrochemistry, Environmental Microbiology and Soil Conservation, Institute of Natural Resources and Agricultural Biology, IRNAS-CSIC, 41012 Seville, Spain
* Correspondence: saiz@irnase.csic.es

Abstract: Understanding the dynamics and spatial distribution of gases in the subterranean atmospheres is essential to increase the reliability of carbon balances in karst ecosystems or the paleoclimate reconstructions based on cave deposits. This scientific information is also very valuable for cave managers to ensure the safety of visitors and the conservation of the subterranean heritage. Through a comprehensive monitoring of the main air parameters in a shallow temperate cave, we decipher the physical drivers and mechanisms involved in the CO_2 and radon exchange between the cave and the outer atmosphere, and how this process is triggered by the changes of local weather. Our results reveal that the biphasic infiltration (water plus air) in the network of penetrative structures from the overlying soil and host rock exercise remarkable control over the cave environment, delaying the thermal response of the cave air to the outer climate-driven changes and also the gaseous transfer between the cave atmosphere and the exterior. The cave location concerning the karstified outcrop determines that this subterranean site acts as a gas emitter during summer, which is contrary to what happens in many other caves. Prominent gas entrapment at a micro-local level is also registered in some upper galleries.

Keywords: greenhouse gases; vadose zone; monitoring; ventilation; karst; critical zone

Citation: Fernandez-Cortes, A.; Martin-Pozas, T.; Cuezva, S.; Cañaveras, J.C.; Saiz-Jimenez, C.; Sanchez-Moral, S. Unraveling the Drivers Controlling the Transient and Seasonal CO_2 Dynamic in a Shallow Temperate Cave. *Geosciences* **2022**, *12*, 335. https://doi.org/10.3390/geosciences12090335

Academic Editors: Suzanne Golding and Jesus Martinez-Frias

Received: 30 July 2022
Accepted: 5 September 2022
Published: 7 September 2022

1. Introduction

Subterranean karst environments can seasonally operate as sinks/reservoirs or emitters/sources of gases, some of them greenhouses involved in the carbon and nitrogen cycles (CO_2, CH_4 or N_2O). Under the context of climate change, gas monitoring in caves can contribute to a better understanding of the role that climatic factors play on their fluxes in the vadose zone of karst, as a particular ecosystem within the Critical Zone.

The CO_2-storage capacity of the vadose zone of karst system is widely known. In terms of the CO_2 balance on terrestrial ecosystems, some studies have estimated a net annual contribution of carbonate rocks ranging from three to eight percent of the total annual atmospheric CO_2 sink [1,2]. Other approximations estimate that the worldwide karst carbon storage in the gas phase could represent 60% of the annual atmospheric sink [3] or the CO_2 storage in subterranean atmospheres could represent up to 56.2% of the residual land CO_2 sink [4]. Recent estimates report between 2 and 53 PgC in a terrestrial carbon reservoir located in the unsaturated zone of aquifers worldwide [5]. In the context of the net gas exchange between the soil–epikarst and atmosphere, some anomalies of

CO_2 fluxes have been reported, consisting of the dry season's CO_2 emissions [3]. These anomalies cannot be explained with purely ecophysiological processes, but, on the contrary, other abiotic mechanisms and their drivers appear to be involved: weathering processes (dissolution and precipitation of carbonates [6,7]), subterranean cavity ventilation [8] and upward diffusion from depth [9].

The classic general pattern of CO_2 distribution in the vadose zone of karst entails an increase of levels with depth, reaching a maximum just above the groundwater level [10]. Other studies described some anomalies concerning the distribution and time evolution of the air CO_2 content in the vadose zone of a karst [11]. Benavente et al. [11] reported high CO_2 concentrations of nearly 40,000 ppm with sharp daily and seasonal variations as a consequence of the ascendant or descendant air fluxes or gas diffusion through karst conduits and voids. Carbon dioxide retention (or exchange) is controlled by the interaction between atmosphere, soil and typical vadose attributes, mainly the relative humidity of the soil and air-filled conduits and water content [12].

The seasonal and transient gas variations in the vadose zone controlled by climatic factors and its implication for regional CO_2 budgets still require more specific and locally controlled studies. Caves and other solution openings in the vadose zone of carbonate outcrops are suitable emplacements to study dynamic gases in subterranean atmospheres, in particular carbon dioxide and radon [13–16], among others. The gas transport to the cave atmospheres is controlled largely by diffusion, due to the establishment of a concentration gradient from the subsoil to cave [17]. The gas depletion of the cave atmosphere can also be caused by ventilation (net movement of air masses to the exterior) triggered by barometric pulses or convective circulation of air favored by a thermo-density gradient [18,19]. Caves show different ventilation patterns, ranging from slow drainage at week–month long time scales to hourly and daily fluctuations [20–22].

Here, we conducted spatiotemporal monitoring of the main microclimatic parameters' tracer gases (CO_2 and ^{222}Rn) from a subterranean atmosphere (Ardales Cave, southern Spain), aiming to understand the main factors controlling gas exchange and storage in the shallow and karstified vadose zone during an annual cycle. Some abiotic processes may decouple the magnitude and timing of ecosystem CO_2 exchange from the biological and geochemical CO_2 sources and sinks. These processes are the subsurface storage of CO_2 [23] together with the subsequent de-gassing processes [24,25]. The decoupling in the CO_2 dynamic could be easily observable in cave atmospheres, and we hypothesize that this is largely conditioned by the dimensional and topographical cave features.

2. Materials and Methods

2.1. Studied Site

Ardales Cave area is located on the Internal–External Domain boundary (southern Spain, Figure 1), which constitutes the suture zone of the Betic Cordillera [26]. Specifically, the host rock of Ardales Cave belongs to an isolated outcrop of Triassic dolomitic-marbles from the Bonella–Capellan Unit of the Internal Domain. The cave is located on an elevated hill (647 m a.s.l.) and is unconnected with the surroundings' carbonated outcrops. These carbonates constitute a relict part of a synclinal over a basement of insoluble metapelites. Ardales Cave constitutes a shallow karstic system located on the upper vadose zone, without any remarkably associated springs on the surface. There are only some subterranean water accumulations (Lakes chamber; Figure 1b), all of them well above the water table of the regional aquifer and with a fast response during the rainy periods. Exokarstic landforms are poorly developed; however, the geomorphological structure, combined with the scarce soil cover and the intense fracturing on the surface, entails a foreseeable air connection between the outer atmosphere and most parts of the galleries.

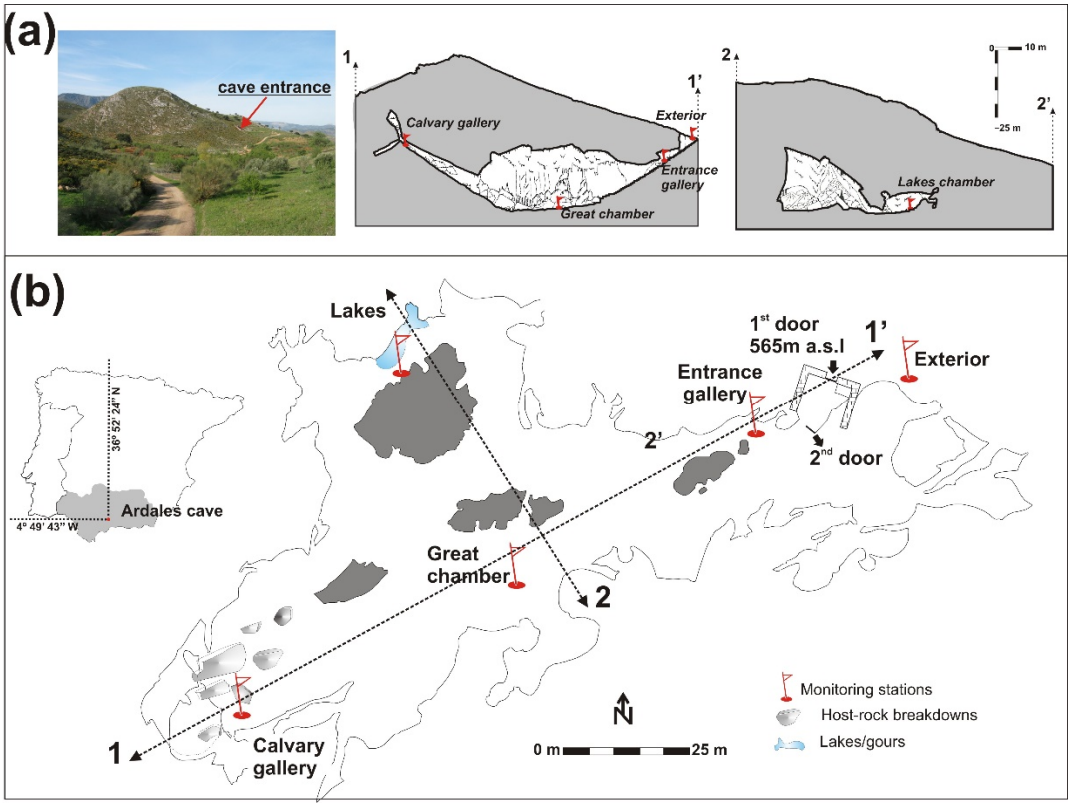

Figure 1. (**a**) Panoramic view of the carbonates outcrop hosting Ardales Cave and cross-sections comparing the cave dimensions with the surface topography. (**b**) Location and cave map with the monitoring stations.

Ardales Cave contains a notable example of Palaeolithic paintings and engravings belonging to the Upper Paleolithic period that date back about 20,000 years [27], and some older ones [28]. The cave has a length of 1.58 km with a maximum difference in height of 34 m. There is a single natural entrance (565 m a.s.l.) with a quasi-hermetic door that remains closed except for some minutes during visits. A hallway was built in 1985 above the cave entrance, just before the door.

Ardales Cave has a controlled visitation (roughly 2600 people/year) with a modified cave entrance that remains closed during periods without visitors. The visitor itinerary reaches the Lakes and Great chambers, and often the Calvary gallery when the group size is less than 15 people (Figure 1). The monthly distribution of the number of visitors is very homogeneous, with an average of 224 people per month. Generally, the cave is not visited during the first two weeks of September. The most common group size is 16 people, with a maximum public attendance from 10 to 12 h GMT and during weekends.

2.2. Cave and Weather Monitoring System

A microenvironmental monitoring system was installed to record the microclimate at different locations of Ardales Cave (the Entrance gallery, the Calvary gallery, the Great and Lakes chambers; Figure 1). The main microclimatic parameters measured within the cave were: temperature, relative humidity, carbon dioxide content of the air and barometric pressure. Measurements were taken at 1 m above the ground and recorded every 5 min during an annual cycle (November–October). Each monitoring station consists of a set of OPUS-200 two-channel datalogger/transmitters (Lufft, Fellbach, Germany), used for resistance, current and voltage measurements with high accuracy. A set of special sensors were installed for the narrow range of measurements expected. Temperature and relative humidity of the air were measured by a Lufft humidity and temperature probe (model 8160.TFF10), which combines a Pt1000 temperature sensor (measuring range −30 to 70 °C,

accuracy ±0.2 °C and resolution 0.05 °C) and a capacitive sensor (measuring range 0 to 100% RH, accuracy ±2% and resolution 0.1%). Cave air CO_2 concentration was measured using an infrared absorption sensor (Lufft 8520) configured over the range 0–3000 ppm, with an accuracy of ±2% of reading and resolution of ±1 ppm (operating range 0–45 °C and avoiding condensation with a vent microsystem). A capacitive ceramic sensor (Lufft 8355.03) measured the absolute pressure of air over the range 600–1100 mbar, with an accuracy of ±0.5 mbar for 20 °C, and 0.1 mbar resolution.

The radon concentration in air (^{222}Rn, Bq/m^3) was hourly measured at the Entrance and Calvary galleries using two Radim 5WP radon monitors (GT-Analytic KG, Innsbruck, Austria). The concentration of radon is determined by measuring in time the α-activity of the decay products of the conversion of radon, collected from the detection chamber on the surface of a Si-semiconductor detector by an electric field. The lowest activity detectable is 80 Bq/m^3, for 1-h measurements with a statistical error equal to ±20%, and the maximum is 150 kBq/m^3. The instrument response is 0.4 (imp/h)/(Bq/m^3). This equipment was calibrated periodically with month-round measurements using solid-state nuclear track detectors (Kodalpha radon dosimeters with a LR115 cellulose nitrate film), with a sensitivity of 1.5–2.4 nuclear track/cm$_2$ for a radon exposure of 1 kBq·h/m^3 and maximum exposure of 70 MBq·h/m^3.

Periodic calibration of the microclimatic series was carried out using a 1521 Handheld Thermometer (Fluke, Hart Scientific, Everett, WA, USA) with an accuracy of ±0.025 °C at 25 °C and temperature Resolution of 0.001 °C. Relative humidity was checked using a temperature–RH combined probe Hygropalm 1 (Rotronic, Switzerland), with an accuracy of ±1.5% over a range 0–100% and a digital resolution of 0.1%). A dual-wavelength infrared absorption sensor was used in the case of CO_2 content of air (SenseAir with a measuring range 0–6000 ppm, the accuracy of ±20 ppm or ±3% of reading, whichever is greater, and resolution of 1 ppm). Each handle probe was periodically subjected to a standard and certificated calibration.

Air density was calculated as a secondary parameter to understand cave air aerodynamics. Besides factors such as temperature and pressure, air density is also determined by taking into account the CO_2-rich air and water vapor saturation of the subterranean atmosphere. Air density in a CO_2-enriched cave atmosphere was calculated based on a proportional replacement of the gaseous constituents of air in function of their partial pressures, in accordance with [29].

3. Results

3.1. General Meteorological Conditions and Prevailing Temperature and Humidity in the Cave

A Mediterranean pluviseasonal–oceanic bioclimate with a dry thermomediterranean ombrothermic type [30] dominates the study site. The mean temperature was 17.5 °C, characterized by a strong seasonality with monthly temperature variations ranging from 2.7 °C (December) to 37 °C (July). The mean relative humidity was 66%, displaying a high level of short-term (daily) and seasonal fluctuations with extremely dry conditions during summer and monthly values higher than 90% from December to April (Figure 2). The annual rainfall was 422 mm. The water deficit prevails during most of the year except for occasional and intense rainfalls, higher than 10 mm/day, registered in March–April, October and winter months.

The Entrance gallery is usually the colder area of the cave, with an annual mean temperature of 16.68 °C. The mean value of the air temperature in the cave's inner areas oscillated between 16.84 °C and 16.90 °C (Great and Lakes chambers), rising to 17.49 °C in the highest area (Calvary gallery). The natural seasonal pattern of air temperature in the Calvary gallery ranged in a narrow interval from 17.4 to 17.6 °C. Visitors cause temporary increases of 0.2–0.4 °C in this cave site, in such a way that the maximum values of air temperature in the cave were reached in the Calvary gallery (17.89 °C in April), almost one degree above the temperature in the rest of the cave (Figure 3). This thermal impact of human presence is less evident in the rest of the monitoring stations.

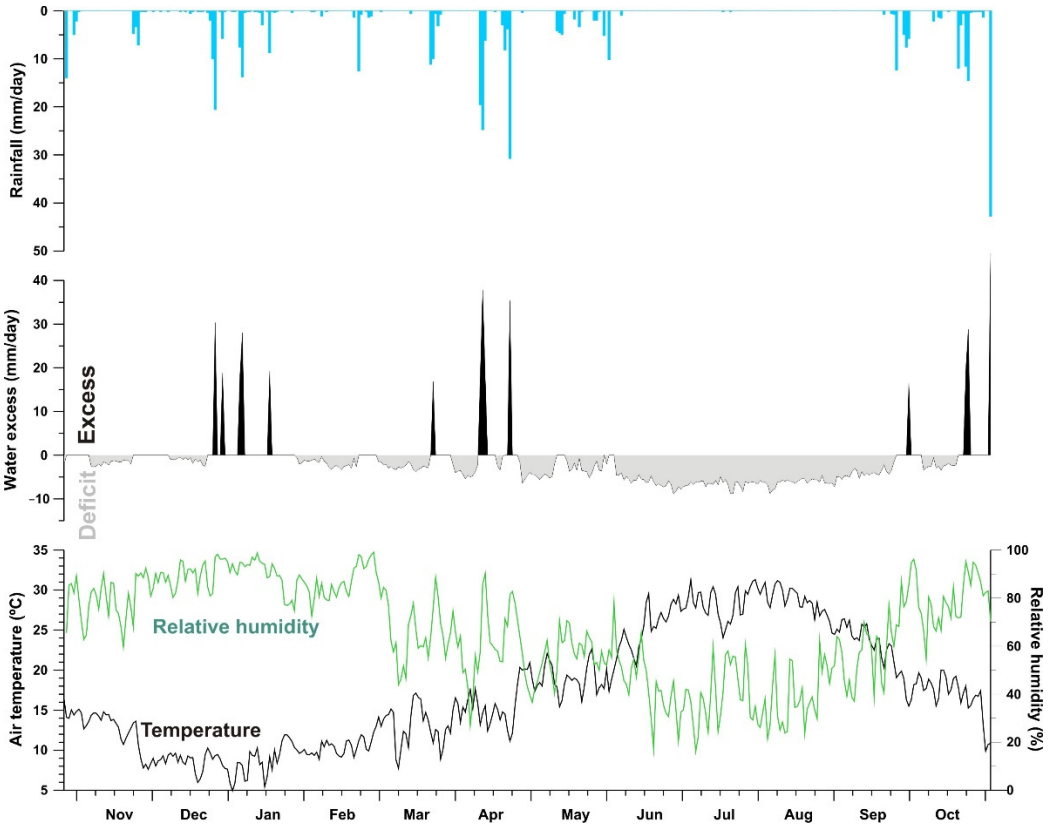

Figure 2. Local daily meteorological conditions during the monitoring period.

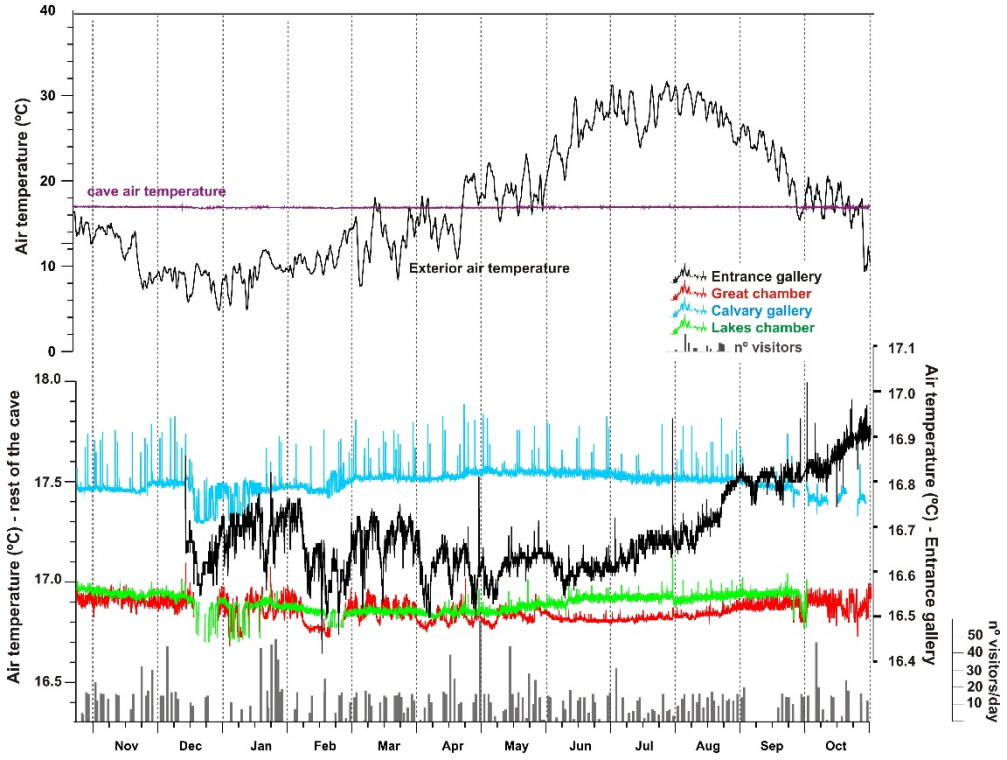

Figure 3. Air temperature at each monitoring station compared to the thermal difference between the exterior and the averaged cave temperature. Daily visits are also plotted to reveal the impacts on air temperature in the Calvary gallery.

The monthly thermal amplitude of cave air was practically constant throughout an annual cycle (around 0.20 °C) except for the Great chamber and the Entrance gallery, where a marked decrease of short-term fluctuations of temperature was registered from May to August.

From May to September, the exterior air temperature was constantly above the cave air temperature, with an opposite pattern during the rest of the year (Figure 3). When the cave air temperature was continually lower than the air temperature of the external atmosphere, the Entrance gallery underwent a fast increase of the mean monthly temperature (+0.26 °C) from June to October. This thermal rise was delayed and smoothed in the deepest areas of the cave; +0.07 °C at the Lakes chamber and +0.08 °C at the Great chamber. These thermal increases during summer and autumn were coeval with a slow downward trend of the temperature at the Calvary gallery (it dropped −0.15 °C from May to October). The air temperature tended to be homogenized along the cave during the late summer and autumn (around 16.90 °C). However, this thermal homogenization was not noticeable at the Calvary gallery, where the air temperature never decreased below 17.3 °C.

The monthly mean temperature decreased to 16.80 °C and 16.85 °C during February in the Great and Lakes chambers, respectively, once the cave air temperature became continuously higher than the air temperature of the external atmosphere (from November–December). During December and January, some short-term and sudden temperature drops were frequently registered in the cave, including both the inner galleries and the highest areas, such as the Calvary gallery. These rapid shifts were coeval to the coldest weather conditions on the exterior, but in the Great chamber and, especially, in the Entrance gallery, they were extended in time during winter and spring months.

The cave atmosphere has constant relative humidity values near saturation. Absolute humidity was calculated from the estimated values of saturated vapor pressures data obtained from the temperature and relative humidity database. It ranges from 14 to 14.5 g/m^3, with lower values in the Entrance gallery and slightly higher values in the Great and Lakes chambers. The extreme values (above 14.8 g/m^3) were continually registered in the Calvary gallery, with almost daily increments reaching up to 15.2 g/m^3 due to visits. Under these humidity saturation conditions of air throughout the cave, the seasonal pattern of the temperature determines the absolute humidity evolution. Therefore, the highest temperature of the Calvary gallery entails the highest absolute humidity values.

The cave atmosphere showed a moderate annual variation of the barometric pressure (±33 mbar) following the barometric fluctuations outside. The mean value of the barometric pressure was 1019 mbar, ranging from 999 to 1034 mbar. The highest fluctuations of air pressure were registered from January to April (>25 mbar). Some short-term shifts in the cave air pressure were detected in April, coinciding with several torrential rainfalls. The lowest monthly variations of air pressure in the cave were registered during summer.

3.2. Gas Composition of the Cave Atmosphere: CO_2 and ^{222}Rn

The mean CO_2 concentration of the cave atmosphere was 1037 ppm, with variations from 630 ppm to 1560 ppm for an annual cycle and considering the averaged CO_2 signal from the four monitoring stations (Figure 4). The minimum CO_2 levels were registered from July to October (lower than 700 ppm), and the maximums were reached from December to March (higher than 1400 ppm). Some data are missing due to instrument failure, especially from November to March in the Calvary gallery and from August to October in the Lakes chamber. Nevertheless, the monitoring records revealed that the CO_2 levels of air were very homogeneous along the cave, with differences between the Entrance gallery and the deepest areas of the cave (Lakes and Great chambers) that hardly reach 100 ppm.

The exception is the CO_2 level at the Calvary gallery, which remained 150–200 ppm above the rest of the cave during the monitoring period. From June to September, the CO_2 level at the Calvary gallery was constantly higher than 740 ppm, and it tended to be at least equal to the rest of the cave during May and October. The CO_2 at the Calvary gallery underwent a daily increase coincidental to the presence of visitors, such as happened with the temperature series. This human impact was not noticeable in other monitoring stations;

thus, the maximum levels above 1000 ppm occurred during summer at the Calvary gallery, whereas the CO_2 concentration rarely exceeded 800 ppm in the rest of cave sites during this season.

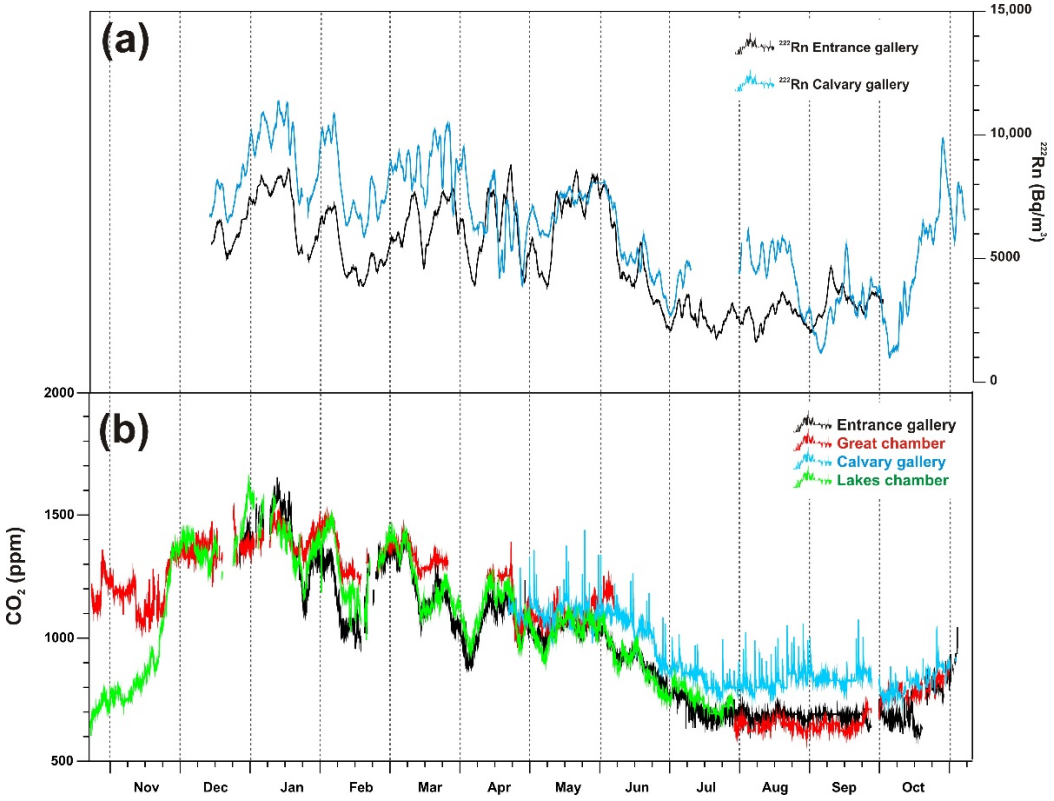

Figure 4. (**a**) Time series of Radon levels (^{222}Rn) and (**b**) CO_2 concentration of cave air at each monitoring station.

The continuous radon monitoring revealed that the averaged concentration of this tracer gas in the cave atmosphere varied from 5050 Bq/m^3 (Entrance gallery) to 6320 Bq/m^3 (Calvary gallery) throughout the year. Some instrument failures caused a lack of data from October to November. The highest differences of ^{222}Rn levels between both areas were registered from January to early April (>2000 Bq/m^3, Figure 4). An additional year-long survey of ^{222}Rn content was carried out in different areas of the cave by using solid-state nuclear track detectors. Some spatially significant differences in annual mean levels were detected (see Figure 1 for locations): 3847 (±77) Bq/m^3 at the Entrance gallery, 4800 (±96) Bq/m^3 at the Great chamber, 7054 (±141) Bq/m^3 at the Calvary gallery, 6420 (±128) Bq/m^3 at Camarin (cul-de-sac part of the Calvary gallery) and 7042 (±141) Bq/m^3 at the Lakes chamber.

The Entrance gallery registered minimum values of ^{222}Rn during the summer season (from July to August), with monthly averaged values around 2600 Bq/m^3 and absolute minimums below 1500 Bq/m^3. The minimum ^{222}Rn levels were delayed until early fall in the Calvary gallery, reaching the lowest monthly mean in September (3050 Bq/m^3) and the absolute minimums during the first days of October (420 Bq/m^3) once the temperature of the cave tended to be equal to the outside atmosphere (Figure 4).

The monthly averaged ^{222}Rn content at the Entrance gallery reached maximum values above 6000 Bq/m^3 during December–January and March–May. Absolute maximums above 9000 Bq/m^3 were registered during January, April and June at the Entrance gallery. As far as the Calvary gallery is concerned, the monthly averaged ^{222}Rn content reached maximum values above 7500 Bq/m^3 from December to March. During these months, the absolute maximum values exceeded 10,500 Bq/m^3 at the Calvary gallery. Maximum monthly variations were registered during June at the Entrance gallery (±7080 Bq/m^3), coinciding

with a prevailing downward trend up to reaching minimum radon levels during summer. At the Calvary gallery, the maximum monthly fluctuation (10,400 Bq/m^3) was reached during October due to a remarkable upward trend in the radon level.

4. Discussion

4.1. Drivers and Seasonal Pattern of Cave Gases

Tracer gas concentration rises when the cave is poorly ventilated, and it decreases during enhanced air exchange with the outside [22]. The similar pattern of variations between ^{222}Rn and CO_2 inside Ardales Cave (Figure 4) indicates that the ventilation process determines variations in both gases. The variability of CO_2 and ^{222}Rn is characterized by low summer and high winter levels, an opposite pattern regarding many other caves where the prevailing loss of CO_2 and ^{222}Rn of the cave atmosphere happens during winter [31] (and references therein).

The thermal and density gradients between the exterior and cave atmosphere, relative humidity at the exterior and rainfalls are the key parameters that allow distinguishing the two stages (cave ventilation versus isolation) over an annual cycle (Figure 5). The alternation and intensity of both stages are detailed in each season as follows:

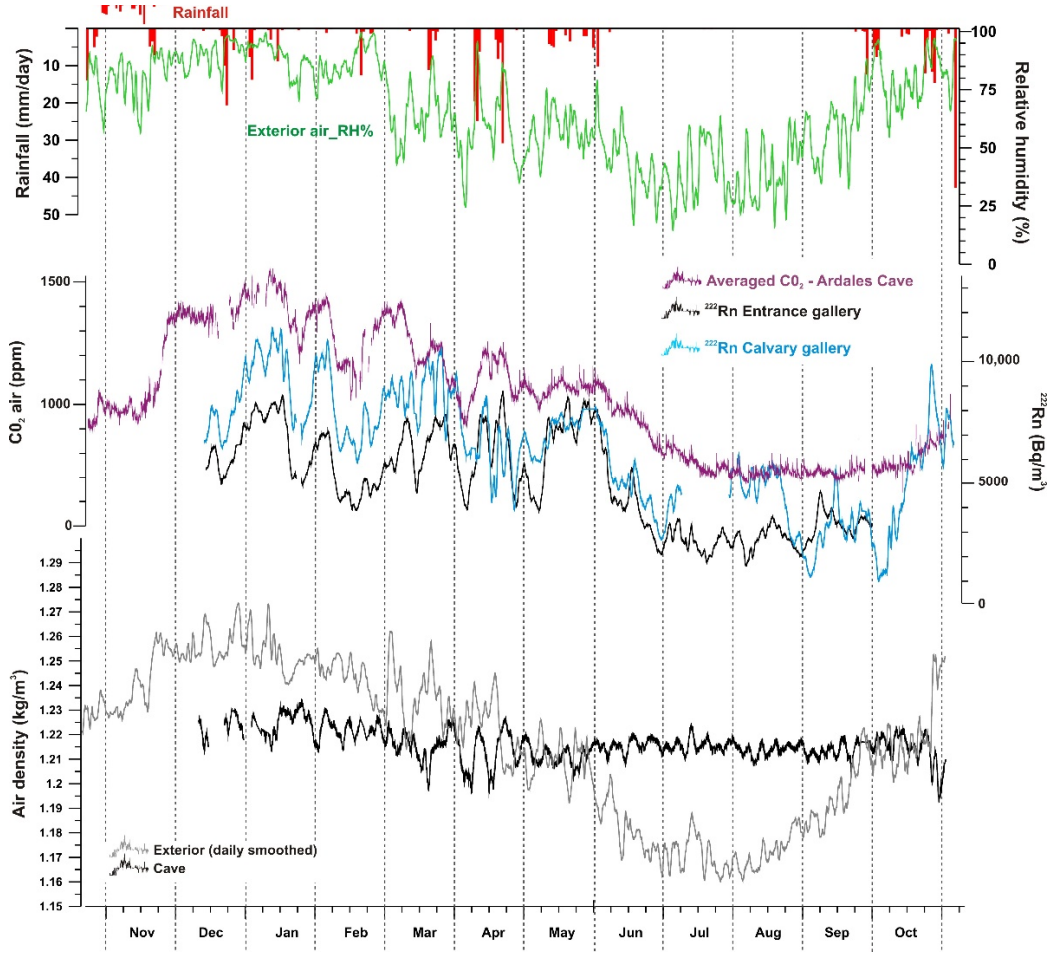

Figure 5. Time series of Radon levels (^{222}Rn) and averaged CO_2 concentration of cave air, controlled by the following key parameters: air density difference between the exterior and cave atmosphere, relative humidity at the exterior and rainfalls.

Winter season: from the end of November to early March, the external air temperature is considerably lower than the cave air temperature and, hence, a negative air-density gradient is established between the exterior and the cave atmosphere. During this period,

rainfall accounts for 25% of the total annual rainfall; however, the monthly mean relative humidity at the exterior is always above 85%, and the minimum values never drop below 50%. Under these environmental conditions, the high water reservoir in the scarce soil cover and the host rock of the vadose zone immediately over the cave leads to the isolation of the cave atmosphere, and the average CO_2 and ^{222}Rn content in the cave air reach maximum levels. The water saturation within the soil pore system and fissures of host rock determines gas exchange processes (ventilation/charge) between the outer atmosphere and the voids and cavities from the endokarst. Condensation and seepage water regulate the available space within the soil pores and the interconnected fissures from the host rock, which leads to a reduction in the gaseous diffusion coefficient of these microenvironments [32]. After rainfall episodes or prolonged high humidity conditions, the connection between the exterior atmosphere and underground cavities is hindered due to a rise in the water content, which is responsible for the closure of this overlying membrane comprised of soil and host rock. Other studies inferred the CO_2 flux using box modeling and confirmed an opposite relationship between water excess and reduced CO_2 flux into large volume compartments from Chauvet-Pont d'Arc Cave [33], i.e., contrary to that observed in Ardales Cave. In this way, CO_2 concentration in this cave systematically increased during periods of water deficit, when CO_2 probably flows from the vadose zone surrounding the cave through highly connected, dense, and air-filled cracks. A redistribution of the airflow through larger, open, and non-saturated pathways may obscure the significance of the effect of gas exchange limitation or blocking between the cave and the exterior due to the water saturation of the airflow and infiltration water pathways [34]. CO_2 can be also pushed towards the cave by the water filling up the rock porosity [35] and, in some sites, water may degas in the cave and fill it up with CO_2 [36]. Other studies even suggest a reverse CO_2 pathway, i.e., the subterranean CO_2 pool and its ventilation is the main source of soil CO_2, accounting for up to 80% of the soil gas during cold periods [37].

Spring season: the period from March to May matches the rainiest period of the annual cycle (39% of the total annual rainfall), together with autumn, with frequent, intense rainfalls. These weather instabilities entail drastic shifts in relative humidity in the exterior atmosphere, especially during March and April. Overall, during this quarter, the monthly mean relative humidity at the exterior drops up to 50–65%, with minimum values between 10% and 30%. The increases of air temperature during this period, with the general downward trend and short-term drops of the humidity conditions at the exterior, favor the evaporation process on the carbonates outcrop embracing the cave. It provokes partial air filling of the porous and fissures system and, therefore, increases the gas exchange with the outer atmosphere. Consequently, the tracer gases of the cave air (CO_2 and ^{222}Rn) reach moderate levels because of an incipient ventilation process of the cave atmosphere. The emission of gases by cave ventilation requires an open double-membrane system (host rock and soil) through which gas diffusion mainly can take place. This mechanism is primarily triggered during the warm, dry periods, and it was already reported to explain "anomalous" CO_2 fluxes measured over karst ecosystems at the surface by using the eddy-covariance technique [12] and the daily and seasonal variations of CO_2 by the real-time monitoring of the cave atmosphere [17,19,38]. Similar behaviour has been observed in other porous materials due to the clogging of pores (closed) by water condensation with increasing relative humidity, which provokes the increase of radon concentration in shallow subterranean environments [39].

Summer season: from June the air temperature at the exterior drastically rises (+10 °C) and reaches maximum values during July, whereas the cave air temperature remains practically constant during early summer (+0.05 °C). This new configuration of the thermal relationship between the cave and the outside involves an inversion of the air density gradient, with colder and denser subterranean air. Simultaneously, the drought conditions prevail during this summer quarter, with a significant lack of rainfall (0.3% of the total annual) and a monthly mean relative humidity below 50%, with extreme values lower than 10%. Under these environmental conditions, widespread evapotranspiration provokes the

drying of the scarce soil and an increase in the percentage of air-filled cracks and fissures of the overlying host rock. A net exchange of air with the outer atmosphere is established, especially through the deepest and well-connected areas with the exterior or other galleries near the surface. This air exchange is led by a convective circulation of air because of a density gradient, and this is favored by the special topographical configuration of the cave, located on an elevated promontory. This is described in detail in the following section. Thus, the colder and denser subterranean air descends to the deepest areas of the cave, and it is evacuated through the air-filled penetrative structures. The outer, warmer, and less-dense air seeps through the same network of air-filled penetrative structures, renewing the cave atmosphere at once. These processes entail a ubiquitous depletion of the tracer gas levels of the subterranean atmosphere during summer.

Autumn season: the intense air exchange between the cave and the outside continues over summer and early fall, despite the weather conditions changing at the end of September (relative humidity above 60% and the first rainfalls are registered). In addition, the uninterrupted drop of air temperature at the exterior from August leads to mitigating the differences in air density between the cave and the exterior. During the first days of October, the moisture conditions of the vadose zone immediately above the cave are re-established because of the intense rainfalls (it accounts for 38% of the total annual rainfall). It provokes the partial water filling of the porous and fissures system and, therefore, hides the gas exchange with the outer atmosphere. Therefore, the concentrations of CO_2 and ^{222}Rn of the cave air undergo an upward trend during October and November, reaching high levels at the beginning of December, characteristic of an isolated atmosphere of winter months.

4.2. Cave Topographical and Geomorphological Features Controlling Gases Dynamic

Ardales Cave is above the water table of the local karst aquifer and is topographically elevated and isolated from the surrounding outcrops of carbonates (Figure 1). This geomorphologic setting determines a tridimensional air exchange with the exterior because this process is not intercepted by the deeper water drainage structures linked to the far-off saturated aquifer zone. The prevailing bidirectional air fluxes are established across the cave entrance and the well-connected areas. There is a coeval evolution of CO_2 and ^{222}Rn levels in both elevated and deepest areas. This reveals that the seasonal energy and mass fluxes between the cave atmosphere and the exterior are controlled by a dual mechanism: (1) air density relationship between the cave air and the atmosphere outside as driving force of convective motion of air parcels, and (2) wetting/drying of the double membrane soil–host rock covering the cave and controlling the gas diffusion or net movement of air advection to the exterior by air-filled conduits.

Considering the entire interconnected macropores and fissures of the belowground karst system, the topographical and geomorphological features of Ardales Cave determine two opposite ventilation patterns over an annual cycle (Figure 6). Firstly, during the wetter and colder semester (from November to March), the dense, cold air from the exterior tends to penetrate into the cave, displacing the warmer cave air through the upper parts of the karstic relief where Ardales Cave is located. However, this air renewal is prevented because the cave atmosphere is isolated by water-filling of the pores and fissures network that connect to the external atmosphere. During this period, the cave acts as warm-air trap under thermal disequilibrium with the surrounding outer atmosphere (Figure 6a). This limited air exchange with the exterior entails the cave atmosphere operating as reservoir of tracer gases; thus, the monthly mean CO_2 levels are always above 1000 ppm and ^{222}Rn content reaches maximums levels in the most isolated areas of the cave (monthly mean above 6000 Bq/m^3 in Calvary gallery). The air renewal is forced during short intervals with visits due to the door opening. This effect is marked while the cave air temperature is above the temperature of the external atmosphere. This human-induced ventilation provokes a short-term shift of the air temperature, CO_2 and ^{222}Rn levels in the cave atmosphere, mainly in the Entrance gallery, but also in a smoothed form in the rest of the cave (Figure 3).

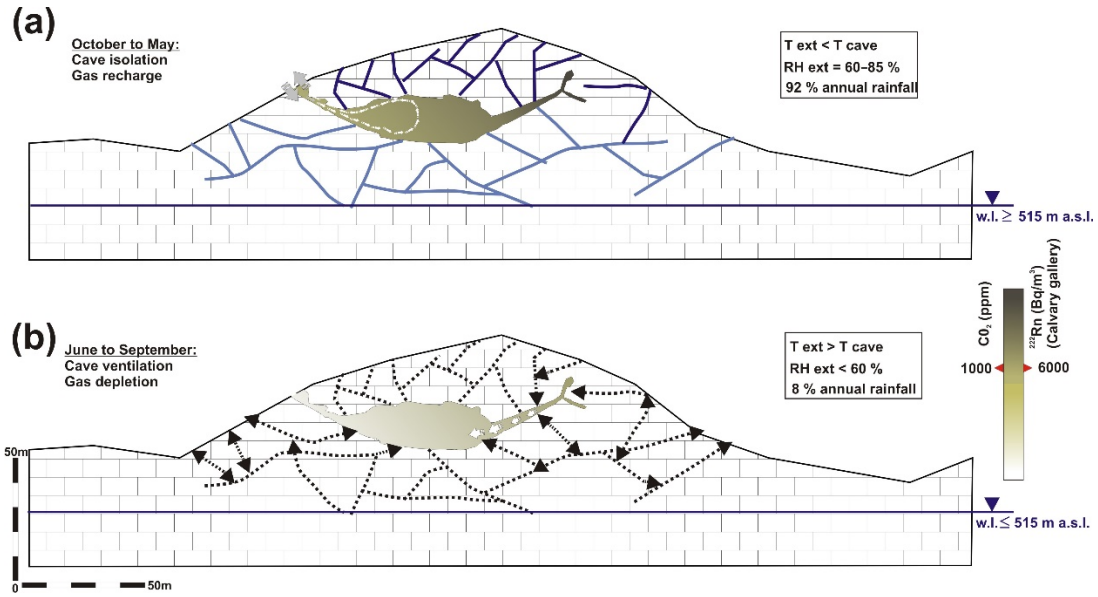

Figure 6. Cross-section of Ardales Cave within the upper vadose zone (heterothermic zone) above the local water table. Two different patterns of cave ventilation are distinguished depending on outdoor weather conditions (see text); (**a**): wet and colder period, and (**b**): drier and warmer period. The idealized network of fissures and conduits network is drawn: (**a**) lower water saturation (blue lines); (**b**) air-filled conduits (dotted lines and arrows).

Secondly, during summer (June–September), at higher external air temperatures, the cold air inside the cave is denser than the outside air and, consequently, it should be trapped inside the cave; consequently, the exchange with the external atmosphere should be blocked. However, the widespread drying process of the overlying soil and host rock provokes an increase in the proportion of air-filled conduits feeding the cave. Accordingly, the inversion of the air density gradient favors the influx of warmer and less dense air parcels from the exterior into the cave, mainly across the open connections located at lower levels of the cave (Figure 6b). The upward inlet of warmer air from the exterior atmosphere is perceived as a growing trend of cave air temperature, from June to the end of September (Figure 3), This temperature rise is registered in each one of the monitoring stations, except for the highest and isolated areas, such as the Calvary Gallery. Simultaneously, the colder and denser air parcels from the upper areas would descend down and be evacuated to the exterior through the deepest galleries of the cave, especially those that are well connected with the outer atmosphere by fractures. The remarkable air exchange with the exterior shows that the cave atmosphere operates as a CO_2 emitter to the exterior during this warm–dry season. This causes the monthly average CO_2 values to descend below 1000 ppm. Likewise, the intense air renewal results in a decrease of ^{222}Rn below 5000 Bq/m^3.

May and October represent transition periods during which the air density gradient is practically absent due to a thermal equilibrium between the cave air and the external atmosphere. This equilibrium involves the aerodynamic stability of the cave atmosphere without any net movement of air parcels induced by the particular cave geomorphology. During both months, the recorded rainfall is 77% of annual precipitation and, therefore, the seepage water would become the main driving force transporting tracer gases into the cave atmosphere.

4.3. The Motionless Atmosphere in the Calvary Gallery; an Example of Gas Trapping

Despite the well-defined seasonal cycles of air renewal of the cave atmosphere, a local microclimatic anomaly is detected in the Calvary gallery. The air parcel from this gallery is involved to a lesser extent in the gas exchange process with the outer atmosphere and surrounding chambers of the cave. This is a higher and near-surface gallery that constantly

traps warmer and less dense air over time. Furthermore, the presence of the highest vapor content under equilibrium conditions allows for a relatively isothermal reaction and contributes to blocking the air movement because the temperature differences are not sufficient to create any eddies. The marked stratification of air over an annual cycle ensures that a hot bubble with CO_2-enriched air is lodged in the Calvary gallery. Only the diffusion through the fissures of the upper host rock can evacuate gases from this end-blinded gallery since the entrance is too far for the activation of convective air circulation.

Air temperature in the upper areas such as the Calvary gallery remains 0.6–0.8 °C higher than in all other areas of the cave all year, without considering the short-term and intermittent increments of temperature because of visits to this gallery. Likewise, under vapor pressure equilibrium of the cave atmosphere and close to 100% relative humidity, the absolute humidity in Calvary gallery remains constant within a narrow range between 14.85 and 14.95 g/m^3 (0.6 g/m^3 above other areas), with almost daily imbalances due to the vapor exhalation of visitors.

The trap of warmer, less dense and CO_2-rich air from the Calvary gallery operates as a motionless atmosphere. Consequently, the seasonal microclimatic fluctuations in this gallery are smoothed compared with the other areas. The air of the Calvary gallery also reacts to sudden and natural shifts of the hygrothermal conditions with some delay, contrary to what has been described in other areas of the cave. Similarly, any long-term drift of air temperature due to the seasonal step pattern of ventilation/isolation of the cave is practically hidden. Nevertheless, the almost daily presence of small groups of visitors in the Calvary gallery provokes short-term increases of temperature and water vapor as well as carbon dioxide contents in this semi-static air parcel [40].

4.4. Observations and Importance for Carbon Balance in Karst and Cave Conservation

Several observations and interpretations can be proposed in terms of the carbon balance in karst areas and the development and management of cave tourism. Firstly, the water content in the vadose zone above the caves must be considered as a key parameter to locally characterize its role as temporal depots or emitters of carbon dioxide under the setting of karst ecosystems. Indeed, if water content decreases, with more frequent dry periods, then even lower CO_2 concentration in cave air can be expected due to active gas exchange with the outer atmosphere. This conceptual model for CO_2 transport works for the case of Ardales Cave, located on a karstic promontory well above the phreatic level, but it would not work for other caves below nearly flat karst outcrops, where the porosity controlling the CO_2 flow is air-filled during dry periods and the input of enriched-CO_2 into the cave is favored [33].

Secondly, carbon dioxide concentration is a key parameter of underground atmospheres for cave heritage preservation since it controls the chemical conditions at the wall and ceiling surfaces. Therefore, the characterization of CO_2 sources and transport modes into and out of the caves is vital for understanding the deterioration processes of the supports hosting the prehistoric engravings and paintings and for monitoring any conservation or remediation measurement. In the case of Ardales Cave, the combination of microclimate monitoring and aerobiological sampling allowed us to detect evident human disturbances in certain cave areas, such as the Calvary gallery, that should be apparently outside the scope of visitors' influence, either due to their remoteness to the tourist pathway or by being briefly visited [40]. The human disturbances in the environmental parameters of this cave gallery with a high density of paintings and engravings should serve as a key control point for the managers of the cave when establishing measures to control access to the cave and aiming to preserve its cultural heritage.

5. Conclusions

Ardales Cave is located in the heterothermic zone of karst where its temperature distribution is subject to heat conduction through the matrix by heat advection or by water and air circulation. There is a thermal disequilibrium with the exterior that prevents the

cave to follow synchronously the local climate fluctuations, causing seasonal energy and mass fluxes between the cave atmosphere and the exterior.

The degree of water saturation in the host rock and soil controls the gas exchange processes between the cave and the outer atmosphere. Wet and rainy weather provokes an intense water filling process within the network of fissures and pores of this double-membrane system, delaying the air gaseous transfer between the cave atmosphere and the exterior. On the contrary, the dry weather conditions cause the partial opening (air filling) of the porous system of the upper soil and the network of host-rock fissures of the vadose zone; consequently, air exchange between the cave and the exterior atmosphere is favored.

Our results reveal that the magnitude and direction of gas exchange fluxes between the upper vadose zone of karst and the external atmosphere are mainly controlled by the geometry and topographical and geomorphological position of the cave in relation to the surface. These features also affect the gas mobility in the cave atmosphere and how the meteorological conditions trigger the ventilation process. These factors determine that this subterranean site acts as a gas emitter during summer, i.e., with an opposite pattern to many other caves where the prevailing depletion of CO_2 and ^{222}Rn happens during winter. There are also some spatial anomalies in this cave, such as the gas entrapment in the Calvary gallery. At this end-blinded gallery with an upward slope, there is CO_2 and radon accumulation near the gas source, whatever the origin (gas diffusion from the near soil and host rock or human breathing), and this gas trapping is favored by a coeval air thermal stratification that creates a motionless and warm air mass.

The results and spatiotemporal findings from our research also provide new insights in this research line but also for better designing, operating, and maintaining other underground facilities located in the vadose zone, as well as for identifying and prospecting suitable subterranean environments for gas storage. The obtained results also have a direct application for assessing the quantitative transfer functions from external weather/climate to speleothems records to establish paleo-climate interpretations. In the particular case of Ardales Cave, they would constitute a valuable database for the conservation of the geological heritage and the exceptional prehistoric engravings and paintings of this subterranean site.

Author Contributions: Conceptualization, A.F.-C. and S.S.-M.; methodology, A.F.-C., S.S.-M. and S.C.; formal analysis, A.F.-C., S.S.-M. and S.C.; investigation, A.F.-C., S.S.-M., T.M.-P., S.C., J.C.C., C.S.-J.; writing—original draft preparation, A.F.-C. and S.S.-M.; writing—review and editing, A.F.-C., S.S.-M. and C.S.-J.; project administration, A.F.-C. and S.S.-M.; funding acquisition, A.F.-C., S.S.-M., J.C.C. and C.S.-J. All authors have read and agreed to the published version of the manuscript.

Funding: This research was funded by the Spanish Ministry of Science, Innovation through project PID2019-110603RB-I00, MCIN/AEI/FEDER UE/ 10.13039/501100011033, and PID2020-114978GB-I00.

Data Availability Statement: Not applicable.

Acknowledgments: The Museum of Prehistory from Ardales Cave (Malaga, Spain) and its staff are acknowledged for their administrative and technical support. The authors wish to acknowledge the professional support of the CSIC Interdisciplinary Thematic Platform Open Heritage: Research and Society (PTI-PAIS).

Conflicts of Interest: The authors declare no conflict of interest.

References

1. Gombert, P. Role of karstic dissolution in global carbon cycle. *Glob. Planet. Chang.* **2002**, *33*, 177–184. [CrossRef]
2. Liu, Z.; Dreybrodt, W.; Wang, H.J. A possible important CO_2 sink by the global water cycle. *Chin. Sci. Bull.* **2008**, *53*, 402–407. [CrossRef]
3. Serrano-Ortiz, P.; Roland, M.; Sanchez-Moral, S.; Janssens, I.A.; Domingo, F.; Godderis, Y.; Kowalski, A.S. Hidden, abiotic CO_2 flows and gaseous reservoirs in the terrestrial carbon cycle: Review and perspectives. *Agric. Forest Meteorol.* **2010**, *150*, 321–329. [CrossRef]
4. Fernandez-Cortes, A.; Cuezva, S.; Garcia-Anton, E.; Alvarez-Gallego, M.; Pla, C.; Benavente, D.; Cañaveras, J.C.; Calaforra, J.M.; Mattey, D.P.; Sanchez-Moral, S. Changes in the storage and sink of carbon dioxide in subsurface atmospheres controlled by climate-driven processes: The case of the Ojo Guareña karst system. *Environ. Earth. Sci.* **2015**, *74*, 7715–7730. [CrossRef]

5. Baldini, J.U.L.; Bertram, R.A.; Ridley, H.E. A first approximation of the Earth's second largest reservoir of carbon dioxide gas. *Sci. Total Environ.* **2018**, *616–617*, 1007–1013. [CrossRef]
6. Emmerich, E.W. Carbon dioxide fluxes in a semiarid environment with high carbonate soils. *Agric. Forest Meteorol.* **2003**, *116*, 91–102. [CrossRef]
7. Mielnick, P.; Dugas, W.A.; Mitchell, K.; Havstad, K. Long-term measurements of CO_2 flux and evapotranspiration in a Chihuahuan desert grassland. *J. Arid. Environ.* **2005**, *60*, 423–436. [CrossRef]
8. Kowalski, A.S.; Serrano-Ortiz, P.; Janssens, I.A.; Sanchez-Moral, S.; Cuezva, S.; Domingo, F.; Alados-Arboledas, L. Can flux tower research neglect geochemical CO_2 exchange? *Agric. Forest Meteorol.* **2008**, *148*, 1045–1054. [CrossRef]
9. Walvoord, M.A.; Striegl, R.G.; Prudic, D.E.; Stonestrom, D.A. CO_2 dynamics in the Amargosa desert: Fluxes and isotopic speciation in a deep unsaturated zone. *Water Resour. Res.* **2005**, *41*, W02006. [CrossRef]
10. Wood, W.W. Origin of caves and other solution openings in the unsaturated (vadose) zone of carbonate rocks: A model for CO_2 generation. *Geology* **1985**, *13*, 822–824. [CrossRef]
11. Benavente, D.; Vadillo, I.; Carrasco, F.; Soler, A.; Linan, C.; Moral, F. Air carbon dioxide contents in the vadose zone of a Mediterranean karst. *Vadose Zone J.* **2010**, *9*, 126–136. [CrossRef]
12. Cuezva, S.; Fernandez-Cortes, A.; Benavente, D.; Serrano-Ortiz, P.; Kowalski, A.S.; Sanchez-Moral, S. Short-term CO_2(g) exchange between a shallow karstic cavity and the external atmosphere during summer: Role of the surface soil layer. *Atmos. Environ.* **2011**, *45*, 1418–1427. [CrossRef]
13. Perrier, F.; Richon, P.; Gautam, U.; Tiwari, D.R.; Shrestha, P.; Sapkota, S.N. Seasonal variations of natural ventilation and radon-222 exhalation in a slightly rising dead-end tunnel. *J. Environ. Radioact.* **2007**, *97*, 220–235. [CrossRef] [PubMed]
14. Frisia, S.; Fairchild, I.J.; Fohlmeister, J.; Miorandi, R.; Spoetl, C.; Borsato, A. Carbon mass-balance modelling and carbon isotope exchange processes in dynamic caves. *Geochim. Cosmochim. Acta* **2011**, *75*, 380–400. [CrossRef]
15. Mattey, D.P.; Atkinson, T.C.; Barker, J.A.; Fisher, R.; Latin, P.; Durrell, R.; Ainsworth, M. Carbon dioxide, ground air and carbon cycling in Gibraltar karst. *Geochim. Cosmochim. Acta* **2016**, *184*, 88–113. [CrossRef]
16. Garcia-Anton, E.; Cuezva, S.; Fernandez-Cortes, A.; Alvarez-Gallego, M.; Pla, C.; Benavente, D.; Canaveras, J.C.; Sanchez-Moral, S. Abiotic and seasonal control of soil-produced CO_2 efflux in karstic ecosystems located in Oceanic and Mediterranean climates. *Atmos. Environ.* **2017**, *164*, 31–49. [CrossRef]
17. Garcia-Anton, E.; Cuezva, S.; Fernandez-Cortes, A.; Benavente, D.; Sanchez-Moral, S. Main drivers of diffusive and advective processes of CO_2-gas exchange between a shallow vadose zone and the atmosphere. *Int. J. Greenh. Gas. Con.* **2014**, *21*, 113–129. [CrossRef]
18. Bourges, F.; Genthon, P.; Mangin, A.; d'Hulst, D. Microclimates of l'Aven d'Orgnac and other French limestone caves (Chauvet, Esparros, Marsoulas). *Int. J. Climatol.* **2006**, *26*, 1651–1670. [CrossRef]
19. Fernandez-Cortes, A.; Sanchez-Moral, S.; Cuezva, S.; Benavente, D.; Abella, R. Characterization of trace gases' fluctuations on a low energy cave (Castañar de Ibor, Spain) using techniques of entropy of curves. *Int. J. Climatol.* **2011**, *31*, 127–143. [CrossRef]
20. Fernandez-Cortes, A.; Sanchez-Moral, S.; Cuezva, S.; Cañaveras, J.C.; Abella, R. Annual and transient signatures of gas exchange and transport in the Castañar de Ibor cave (Spain). *Int. J. Speleol.* **2009**, *38*, 153–162. [CrossRef]
21. Milanolo, S.; Gabrovsek, F. Analysis of carbon dioxide variations in the atmosphere of Srednja Bijambarska Cave, Bosnia and Herzegovina. *Bound. Layer Meteor.* **2009**, *131*, 479–493. [CrossRef]
22. Kowalczk, A.J.; Froelich, P.N. Cave air ventilation and CO2 outgassing by radon-222 modeling: How fast do caves breathe? *Earth Planet. Sci. Lett.* **2010**, *289*, 209–219. [CrossRef]
23. Richter, D.D.; Markewitz, D. How deep is soil? Soil, the zone of the earth's crust that is biologically active, is much deeper than has been thought by many ecologists. *BioScience* **1995**, *45*, 600–609. [CrossRef]
24. Morner, N.A.; Etiope, G. Carbon degassing from the lithosphere. *Glob. Planet. Chang.* **2002**, *33*, 185–203. [CrossRef]
25. Weisbrod, N.; Dragila, M.I.; Nachshon, U.; Pillersdorf, M. Falling through the cracks: The role of fractures in Earth–atmosphere gas exchange. *Geophys. Res. Lett.* **2009**, *36*, L02401. [CrossRef]
26. Martin-Algarra, A.; Mazzoli, S.; Perrone, V.; Rodríguez-Cañero, R.; Navas-Parejo, P. Variscan Tectonics in the Malaguide Complex (Betic Cordillera, Southern Spain): Stratigraphic and structural Alpine versus Pre-Alpine constraints from the Ardales Area (Province of Malaga). I. Stratigraphy. *J. Geol.* **2009**, *117*, 241–262. [CrossRef]
27. Marti, A.P.; Zilhão, J.; d'Errico, F.; Cantalejo-Duarte, P.; Dominguez-Bella, S.; Fullola, J.M.; Weniger, G.C.; Ramos-Muñoz, J. The symbolic role of the underground world among Middle Paleolithic Neanderthals. *Proc. Natl. Acad. Sci. USA* **2021**, *118*, e2021495118. [CrossRef]
28. Hoffmann, D.L.; Standish, C.D.; Garcia-Diez, M.; Pettitt, P.B.; Milton, J.A.; Zilhão, J.; Alcolea-Gonzalez, J.J.; Cantalejo-Duarte, P.; Collado, H.; de Balbin, R.; et al. U-Th dating of carbonate crusts reveals Neandertal origin of Iberian cave art. *Science* **2018**, *359*, 912–915. [CrossRef]
29. Cuezva, S. Dinámica Microambiental de un Medio Kárstico Somero (Cueva de Altamira, Cantabria): Microclima, Geomicrobiología y Mecanismos de Interacción Cavidad-Exterior. Ph.D. Thesis, Universidad Complutense de Madrid, Madrid, Spain, May 2018.
30. Rivas-Martínez, S.; Rivas-Sáenz, S.; Penas-Merino, A. Worldwide bioclimatic classification system. *Glob. Geobot.* **2011**, *1*, 1–638.
31. James, E.W.; Banner, J.L.; Hardt, B. A global model for cave ventilation and seasonal bias in speleothem paleoclimate records. *Geochim. Geophys. Geosys.* **2015**, *16*, 1044–1051. [CrossRef]

32. Pla, C.; Cuezva, S.; Martinez-Martinez, J.; Fernandez-Cortes, A.; Garcia-Anton, E.; Fusi, N.; Crosta, G.B.; Cuevas-Gonzalez, J.; Canaveras, J.C.; Sanchez-Moral, S.; et al. Role of soil pore structure in water infiltration and CO_2 exchange between the atmosphere and underground air in the vadose zone: A combined laboratory and field approach. *Catena* **2017**, *149*, 402–416. [CrossRef]
33. Bourges, F.; Genty, D.; Perrier, F.; Lartiges, B.; Régnier, E.; François, A.; Leplat, J.; Touron, S.; Bousta, F.; Massault, M.; et al. Hydrogeological control on carbon dioxide input into the atmosphere of the Chauvet-Pont d'Arc cave. *Sci. Total Environ.* **2020**, *716*, 136844. [CrossRef] [PubMed]
34. Kukuljan, L.; Gabrovšek, F.; Covington, M.D.; Johnston, V.E. CO_2 dynamics and heterogeneity in a cave atmosphere: Role of ventilation patterns and airfow pathways. *Theor. Appl. Climatol.* **2021**, *146*, 91–109. [CrossRef]
35. Peyraube, N.; Lastennet, R.; Denis, A.; Malaurent, P.; Houillon, N.; Villanueva, J.D. Determination and quantification of major climatic parameters influencing the CO_2 of Lascaux Cave. *Theor. Appl. Climatol.* **2018**, *133*, 1291–1301. [CrossRef]
36. Covington, M.D. The importance of advection for CO_2 dynamics in the karst critical zone: An approach from dimensional analysis. *Geol. Soc. Am. Spec. Pap.* **2016**, *516*, 113–127. [CrossRef]
37. Krajnc, B.; Ferlan, M.; Ogrinc, N. Soil CO_2 sources above a subterranean cave-Pisani rov (Postojna Cave, Slovenia). *J. Soils Sediments* **2017**, *17*, 1883–1892. [CrossRef]
38. Cao, M.; Lei, J.; He, Q.; Zeng, Z.; Lü, X.; Jiang, Y. Rainfall-driven and hydrologically-controlled variations in cave CO_2 sources and dynamics: Evidence from monitoring soil CO_2, stream flow and cave CO_2. *J. Hydrol.* **2021**, *595*, 126060. [CrossRef]
39. Fernandez-Cortes, A.; Benavante, D.; Cuezva, S.; Cañaveras, J.C.; Alvarez-Gallego, M.; Garcia-Anton, E.; Soler, V.; Sanchez-Moral, S. Effect of water vapour condensation on the radon content in subsurface air in a hypogeal inactive-volcanic environment in Galdar cave, Spain. *Atmos. Environ.* **2013**, *75*, 15–23. [CrossRef]
40. Fernandez-Cortes, A.; Cuezva, S.; Sanchez-Moral, S.; Cañaveras, J.C.; Porca, E.; Jurado, V.; Martin-Sanchez, P.M.; Saiz-Jimenez, C. Detection of human-induced environmental disturbances in a show cave. *Environ. Sci. Pollut. Res.* **2011**, *18*, 1037–1045. [CrossRef]